Proximitized Bilayer Graphene Quantum Dots: Continuum and Atomistic Approaches

Ivan Verstraeten

With David T.S. Perkins, Bert Jorissen, Lucian Covaci, Aires Ferreira

Capri Spring School - 17 April 2026

Universiteit Antwerpen

Computational Materials Modeling
for nanoscience and innovative technologies

Outline

1. Introduction
   - Quantum dots & bilayer graphene
   - Proximitization
2. Model
   - Tight-binding & Continuum
   - SOC-Hamiltonian
   - Confinement
3. Results
   - QD spectrum, with & without SOC

Quantum dots: What & Why?

- What? 3D nanoscale confinement ⟶ “Artificial atoms”

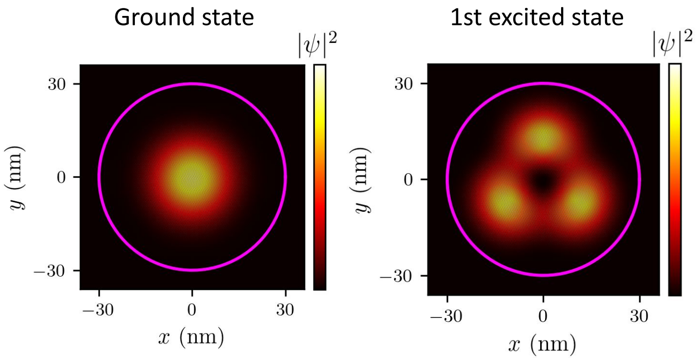

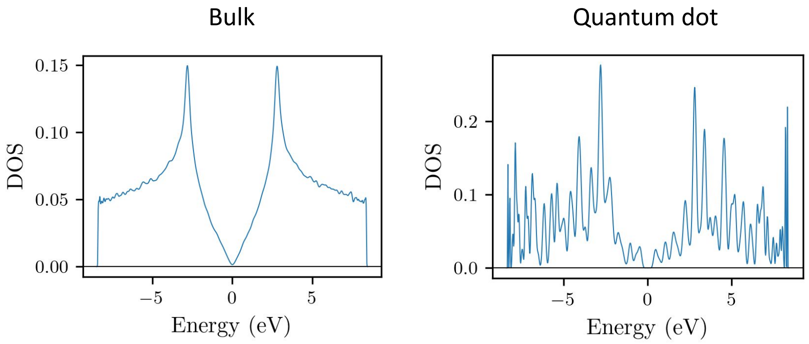

- Discrete energy spectrum ⟶ control over individual electrons
  - Applications: single-electron transistors, single photon sources, **qubits**, etc

Kinds of quantum dots

Nano particle/flake

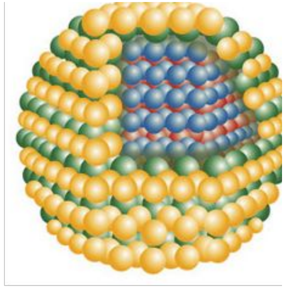

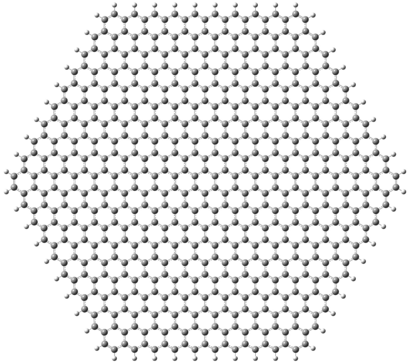

Nanomaterials 2022, *12*(12), 1953

Gating techniques

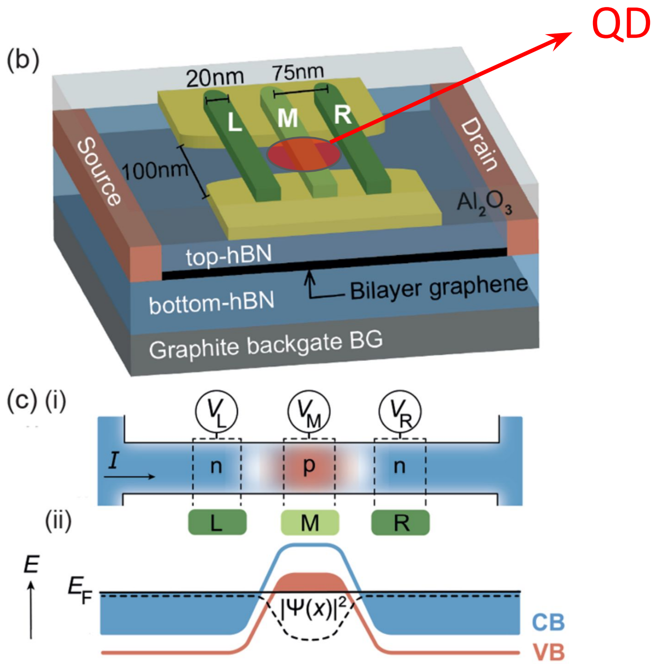

10.1021/acs.nanolett.0c04343

Why bilayer graphene?

Why graphene?

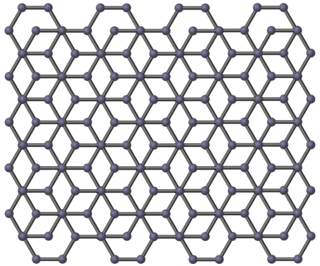

- High lattice symmetry & small atomic number Z
  → low hyperfine & spin-orbit coupling (~50 μeV) → long spin lifetime (T_1 > 200 μs in BLG QD)
  → spintronics & spin-qubits

Intrinsic and Rashba spin-orbit interactions in graphene sheets

Hongki Min*, J. E. Hill, N. A. Sinitsyn, B. R. Sahu, Leonard Kleinman, and A. H. MacDonald

Show more

Phys. Rev. B **74**, 165310 – **Published 9 October, 2006**

DOI: https://doi.org/10.1103/PhysRevB.74.165310

Exp

Article | Open access | Published: 02 September 2021

Spin-valley coupling in single-electron bilayer graphene quantum dots

L. Banszerus, S. Möller, C. Steiner, E. Icking, S. Trellenkamp, F. Lentz, K. Watanabe, T. Taniguchi, C. Volk & C. Stampfer

Nature Communications **12**, Article number: 5250 (2021) | Cite this article

9912 Accesses | **67** Citations | **8** Altmetric | Metrics

Theory of spin-orbit coupling in bilayer graphene

S. Konschuh, M. Gmitra, D. Kochan, and J. Fabian

Show more

Phys. Rev. B **85**, 115423 – **Published 19 March, 2012** | Errata Phys. Rev. B **85**, 109903 (2012); Phys. Rev. B **86**, 119907 (2012)

DOI: https://doi.org/10.1103/PhysRevB.85.115423

Article | Open access | Published: 25 June 2022

Spin relaxation in a single-electron graphene quantum dot

L. Banszerus, K. Hecker, S. Möller, E. Icking, K. Watanabe, T. Taniguchi, C. Volk & C. Stampfer

Nature Communications **13**, Article number: 3637 (2022) | Cite this article

8371 Accesses | **55** Citations | **8** Altmetric | Metrics

Why graphene?

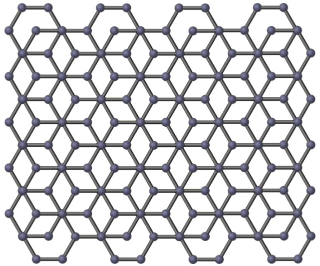

- **Valley** degree of freedom / quantum number: K or K’
    - two non-equivalent points at the edge of the BZ: low energy spectrum

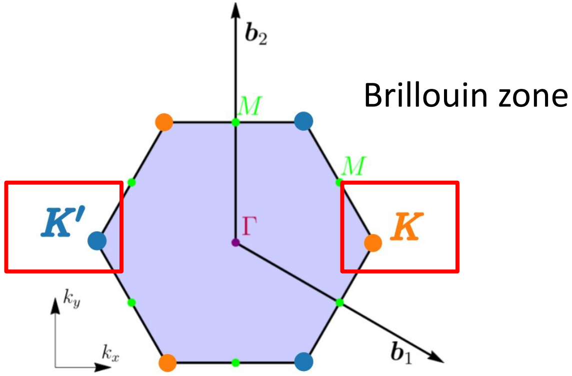

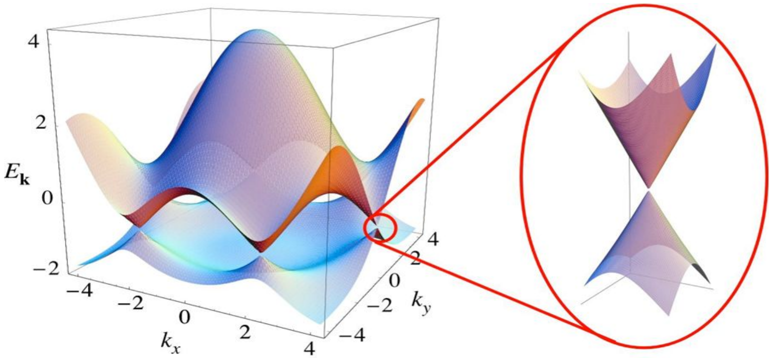

Why a bilayer?

- Monolayer (MLG): low energy spectrum is gapless → electrostatic confinement impossible
- Bilayer (BLG): **tunable band gap** by applying a perpendicular electric field (gating)
  → make a QD using simple gating techniques

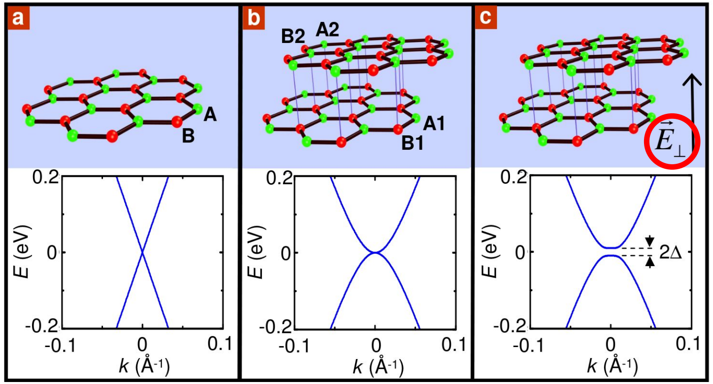

Gate-induced insulating state in bilayer graphene devices

Nature Materials • Article • Open Access • 2008 • DOI: 10.1038/nmat2082

Oostinga, Jeroen B.; Heersche, Hubert B.; Liu, Xinglan; Morpurgo, Alberto F.; Vandersypen, Lieven M. K.
Kavli Institute of Nanoscience, Delft University of Technology, 2600 GA, Delft, PO Box 5046, Netherlands

Nano Letters > Vol 21/Issue 2 > Article

Cite Share Jump to

Subscribed

LETTER | January 15, 2021

Tunable Valley Splitting and Bipolar Operation in Graphene Quantum Dots

Chuyao Tong*, Rebekka Garreis, A… …niguchi, Vladimir Fal'ko, Thomas Ihn, Klaus Ensslin, and Annika Kurzmann

Article | Published: 03 Ju…

Gate-defined … bilayer graph… …ded

M. T. Allen, J. Martin & A. …

Nature Communications …

10k Accesses | 168 Cit…

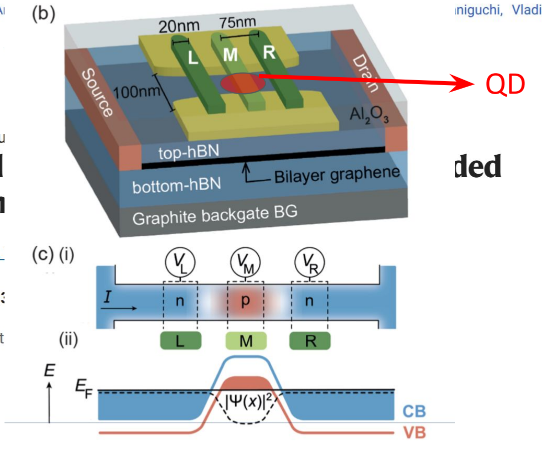

Nano Lett. 2021, 21, 1068−1073

Why a bilayer?

- Strong **valley-Zeeman splitting** ← Band gap + B-field
  - Band gap → Berry curvature → “topological orbital magnetic moment”

No band gap	With band gap

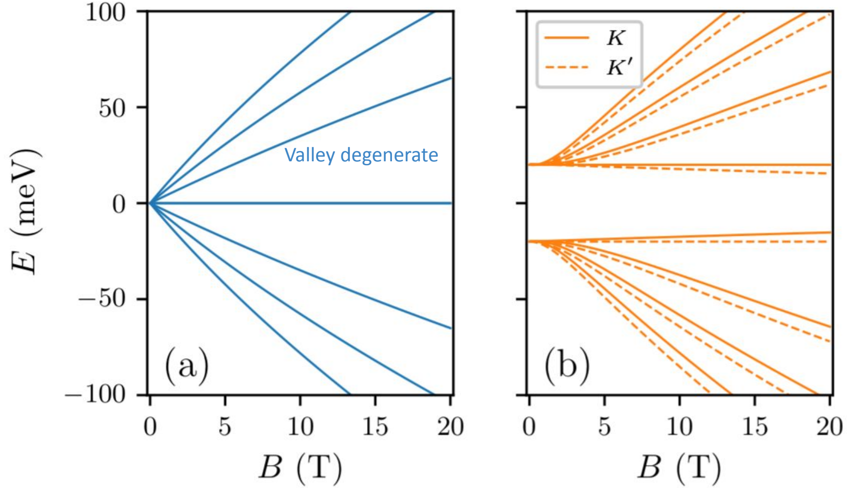

- Layer degree of freedom

Nano Letters > Vol 21/Issue 2 > Article

Subscribed

Cite Share Jump to

LETTER | January 15, 2021

Tunable Valley Splitting and Bipolar Operation in Graphene Quantum Dots

Chuyao Tong*, Rebekka Garreis, Angelika Knothe, Marius Eich, Agnese Sacchi, Kenji Watanabe, Takashi Taniguchi, Vladimir Fal’ko, Thomas Ihn, Klaus Ensslin, and Annika Kurzmann

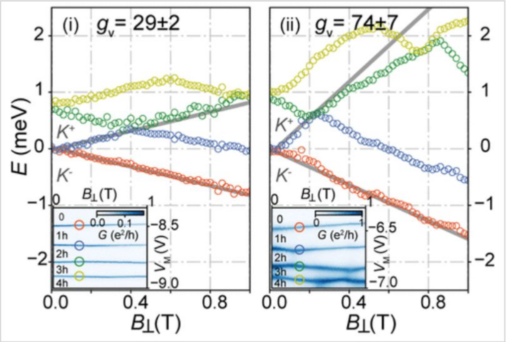

More than an order of magnitude larger than spin-Zeeman!

In summary…

- Graphene
  - Long spin lifetime
  - Valley degree of freedom
- Bilayer graphene
  - Tuneable confinement
  - Strong valley splitting

$\Downarrow$

BLG QD $\longrightarrow$ quantum computing, spintronics, … ?

Missing: control of spin $\longleftarrow$ SOC

Proximitization of the BLG QD

- What?
  - Graphene + TMD (e.g. WSe_2) $\longrightarrow$ enhancement of SOC in graphene: ~10 µeV to ~1-10 meV

Induced spin-orbit coupling in twisted graphene–transition metal dichalcogenide heterobilayers: Twistronics meets spintronics

Alessandro David[1,*], Péter Rakyta[2], Andor Kormányos[2,†], and Guido Burkard[1,‡]

Show more

Phys. Rev. B **100**, 085412 – **Published 8 August, 2019**

DOI: https://doi.org/10.1103/PhysRevB.100.085412

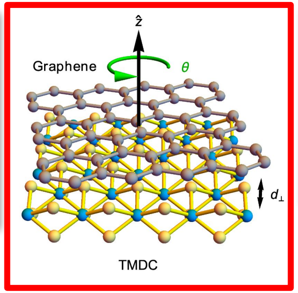

Nano Letters > Vol 17/Issue 12 > Article

Open Access

LETTER | November 27, 2017

Large Proximity-Induced Spin Lifetime Anisotropy in Transition-Metal Dichalcogenide/Graphene Heterostructures

Talieh S. Ghiasi*, Josep Ingla-Aynés, Alexey A. Kaverzin, and Bart J. van Wees

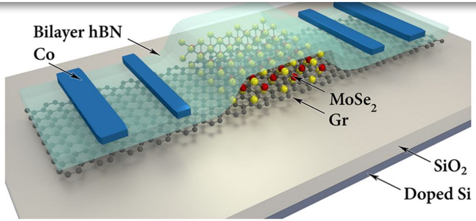

Proximity Effects in Bilayer Graphene on Monolayer WSe_2: Field-Effect Spin Valley Locking, Spin-Orbit Valve, and Spin Transistor

Martin Gmitra and Jaroslav Fabian

Show more

Phys. Rev. Lett. **119**, 146401 – **Published 4 October, 2017**

DOI: https://doi.org/10.1103/PhysRevLett.119.146401

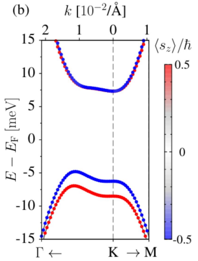

Nano Letters > Vol 25/Issue 33 > Article

Open Access

LETTER | August 7, 2025

Cite Share Jump

Tunable Spin–Orbit Splitting in Bilayer Graphene/WSe_2 Quantum Devices

Jonas D. Gerber*, Efe Ersoy, Michele Masseroni, Markus Niese, Michael Laumer, Artem O. Denisov, Hadrien Duprez, Wister Wei Huang, Christoph Adam, Lara Ostertag, Chuyao Tong, Takashi Taniguchi, Kenji Watanabe, Vladimir I. Fal'ko, Thomas Ihn, Klaus Ensslin, and Angelika Knothe

Proximitization of the BLG QD

- Why?
  - High SOC allows for spin-control
  - SOC will lift degeneracies ⟶ well separated non-degenerate levels

- What about long spin lifetimes?
  - *Anisotropic* spin lifetime
  - Bilayer graphene: tunability!

Nano Letters > Vol 17/Issue 12 > Article

Open Access

LETTER | November 27, 2017

Large Proximity-Induced Spin Lifetime Anisotropy in Transition-Metal Dichalcogenide/Graphene Heterostructures

Talieh S. Ghiasi*, Josep Ingla-Aynés, Alexey A. Kaverzin, and Bart J. van Wees

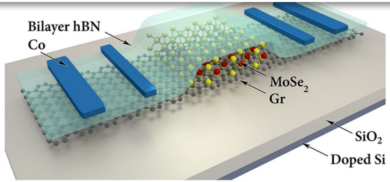

Nano Letters > Vol 25/Issue 33 > Article

Open Access

Cite Share Jump

LETTER | August 7, 2025

Tunable Spin–Orbit Splitting in Bilayer Graphene/WSe_2 Quantum Devices

Jonas D. Gerber*, Efe Ersoy, Michele Masseroni, Markus Niese, Michael Laumer, Artem O. Denisov, Hadrien Duprez, Wister Wei Huang, Christoph Adam, Lara Ostertag, Chuyao Tong, Takashi Taniguchi, Kenji Watanabe, Vladimir I. Fal'ko, Thomas Ihn, Klaus Ensslin, and Angelika Knothe

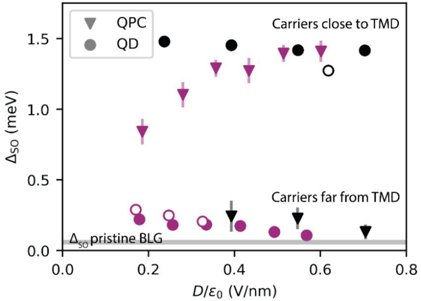

What does this work offer?

- Gaps in the literature
  - Theoretical work on BLG QD lacks atomistic models
  - Recent experiments: *proximitized* BLG QD

    → beyond scope of current models

- This work: address those gaps
  - Theoretical description of *proximitized* BLG QD
    - Analytical continuum model
    - Atomistic tight-binding model

Nano Letters > Vol 25/Issue 33 > Article

Cite Share Jump

Open Access

LETTER | August 7, 2025

Tunable Spin–Orbit Splitting in Bilayer Graphene/WSe_2 Quantum Devices

Jonas D. Gerber*, Efe Ersoy, Michele Masseroni, Markus Niese, Michael Laumer, Artem O. Denisov, Hadrien Duprez, Wister Wei Huang, Christoph Adam, Lara Ostertag, Chuyao Tong, Takashi Taniguchi, Kenji Watanabe, Vladimir I. Fal'ko, Thomas Ihn, Klaus Ensslin, and Angelika Knothe

Nano Letters > Vol 25/Issue 26 > Article

Cite Share Jump to

Subscribed

LETTER | June 18, 2025

Electric-Field-Tunable Spin–Orbit Gap in a Bilayer Graphene/WSe_2 Quantum Dot

H. Dulisch, D. Emmerich, E. Icking, K. Hecker, S. Möller, L. Müller, K. Watanabe, T. Taniguchi, C. Volk, and C. Stampfer*

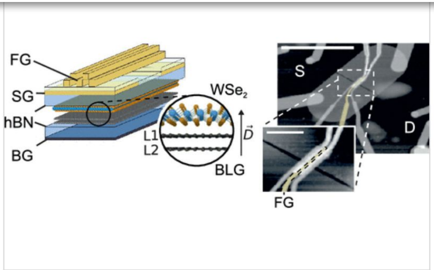

Total Hamiltonian

- Single electron description of the π-bonds of Bernal stacked BLG
- Total Hamiltonian: $H = H_{\mathrm{BLG}} + H_{\mathrm{SOC}} + H_{\mathrm{EM}} + V_{\mathrm{C}}$
  - H_{BLG} : “bare” 8-band BLG Hamiltonian: 1st NN intra-and interlayer hoppings
  - $H_{\mathrm{EM}} = H_U + H_Z$: homogeneous perpendicular electric and magnetic field (B-field: also as modification of momentum: Peierls phase)
  - H_{SOC} : enhanced SOC *as if* proximitized by TMD
  - V_{C} : confinement potential $\longrightarrow$ QD

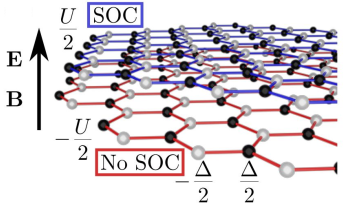

Bird’s-eye view

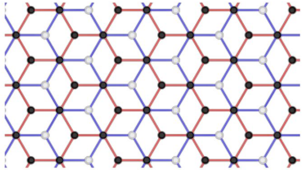

Bernal Stacking

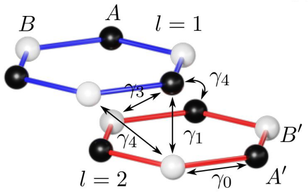

Tight-binding & continuum model
Tight-binding model

- Each atom (p_z-orbital) taken into account
- Large Hamiltonian matrix, constructed using python package "**pyb**inding"
- Numerically diagonalized using ARPACK

- Accurate & flexible: simple implementation of, disorder, symmetry breaking effects, etc
- Computationally expensive: 100,000s lattice sites

$$H = \begin{pmatrix} H_{11} & H_{12} & \cdots & \cdots & H_{1N} \\ H_{21} & H_{22} & \cdots & \cdots & H_{2N} \\ \vdots & \vdots & \ddots & & \vdots \\ \vdots & \vdots & & \ddots & \vdots \\ H_{N1} & H_{N2} & \cdots & \cdots & H_{NN} \end{pmatrix}$$

2N

2N lattice sites

$$H_{ij} = \langle \psi_i | \hat{H} | \psi_j \rangle$$

p_z orbital

First nearest neighbors:

$$\langle \phi_n^{A1} | \hat{H} | \phi_m^{B1} \rangle = \langle \phi_n^{A2} | \hat{H} | \phi_m^{B2} \rangle \equiv -\gamma_0,$$ intralayer

$$\langle \phi_n^{B1} | \hat{H} | \phi_m^{A2} \rangle \equiv \gamma_1,$$ interlayer

Continuum model

- Minimal low-energy continuum model
- Four coupled differential equations
- Limit towards the K-points
  $\longrightarrow$ **valley is built-in quantum number** (in contrast to TB model)
- Continuous real space + circular QD
  $\longrightarrow$ wave functions = eigenfunctions of angular momentum

$$\psi_{s\tau}(\mathbf{r}) = e^{im\theta} \times \left(\phi_{1s\tau}(\rho), ie^{i\theta}\phi_{2s\tau}(\rho), \phi_{3s\tau}(\rho), ie^{-i\theta}\phi_{4s\tau}(\rho)\right)^{\mathrm{T}}$$

  $\longrightarrow$ **angular momentum quantum number** "m" is built-in

- Solved analytically + light numerical self-consistent calculation
- Performed by Dr. David T.S. Perkins, Loughborough University

$$\mathcal{H}_0 = \begin{array}{c} \\ \\ \end{array}\begin{array}{cc} \begin{array}{cccc} \text{A1} & \text{B1} & \text{A2} & \text{B2} \end{array} & \\ \begin{pmatrix} 0 & v\pi_+^\dagger & \gamma_1 & 0 \\ v\pi_+ & 0 & 0 & 0 \\ \gamma_1 & 0 & 0 & v\pi_+ \\ 0 & 0 & v\pi_+^\dagger & 0 \end{pmatrix} & \begin{array}{c} \text{A1} \\ \text{B1} \\ \text{A2} \\ \text{B2} \end{array} \end{array}$$

sublattices

$$\hat{\pi} = \hat{p}_x + i\hat{p}_y, = \frac{\hbar}{i} e^{i\theta}\left(\frac{\partial}{\partial r} + i\frac{1}{r}\frac{\partial}{\partial \theta}\right)$$

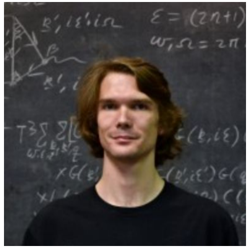

SOC-Hamiltonian

- For each graphene layer separately (no interlayer hoppings)

- Tight-binding:

broken space-inversion symmetry H_{int} broken out-of plane symmetry H_{R}

$$H_{\mathrm{SOC}} = \boxed{\frac{i}{3\sqrt{3}} \sum_{\langle\langle i,j \rangle\rangle} \nu_{ij} \left(\lambda_A \, \hat{a}_i^\dagger s_z \hat{a}_j + \lambda_B \, \hat{b}_i^\dagger s_z \hat{b}_j \right)} + \boxed{\frac{2i}{3} \sum_{\langle i,j \rangle} \left[\lambda \, \hat{a}_i^\dagger \left(\boldsymbol{s} \times \boldsymbol{d}_{ij} \right)_z \hat{b}_j + (b \leftrightarrow a) \right]}$$

- Continuum:

$$H_{\mathrm{SOC}} = \cancel{\boxed{\Delta_{\mathrm{KM}} \tau_z \sigma_z s_z}} + \boxed{\lambda_{\mathrm{sv}} \tau_z \sigma_0 s_z} + \cancel{\boxed{\lambda_{\mathrm{R}} \tau_0 \left(\sigma_x s_y - \sigma_y s_x \right)}}$$

Kane-Mele spin-valley coupling Rashba coupling

$$\Delta_{\mathrm{KM}} = \frac{\lambda_A + \lambda_B}{2}$$ ≃ 42 µeV [(1)]

$$\lambda_{\mathrm{sv}} = \frac{\lambda_A - \lambda_B}{2}$$ < 3 meV [(2)]

λ_{R} < 15 meV [(2)]

[(1)] 10.1103/PhysRevLett.122.046403

[(2)] Nat Commun 14, 3771 (2023)

Confinement: interlayer vs intralayer

- Needed: band gap
  - Transverse electric field (interlayer potential $\boxed{U}$)
    - Max band gap = γ_1
  - Mass term (*intra*layer potential $\boxed{\Delta}$)
    - Max band gap = ∞

Needed to solve continuum model (hard wall)

$\Rightarrow$ use <u>mass term confinement</u>, instead of electric field

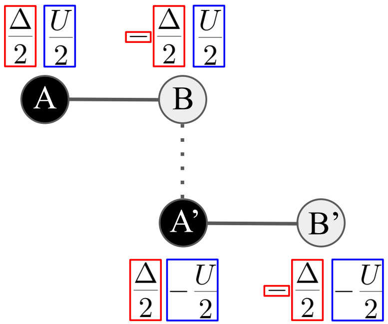

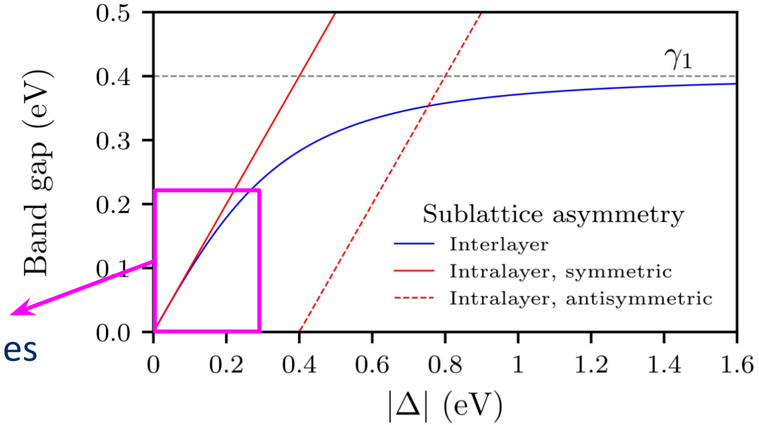

- Mass term emulates an electric field for small energies

No SOC: energy levels vs QD radius

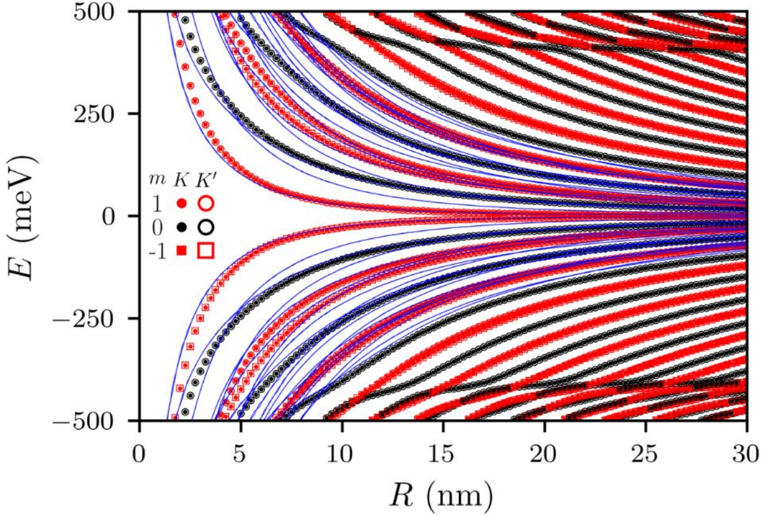

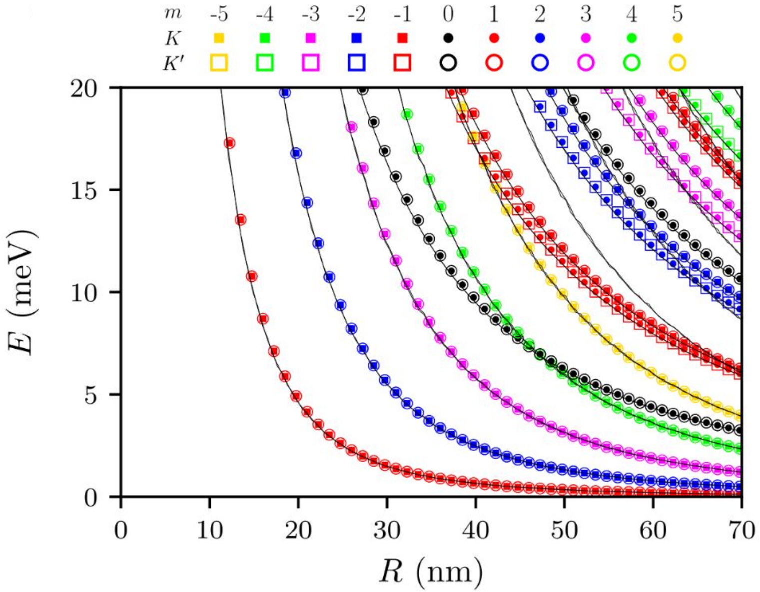

- Monotonic decrease with R (as expected)
- Continuum model matches the tight-binding model very well, better for larger R (as expected)

No SOC: energy levels vs magnetic field

- B = 0: 4-fold degeneracy (no SOC): (K, K')x(↑,↓)
- B ≠ 0: Two splitting mechanisms:
  - Valley-Zeeman (topological orbital moment): ΔE_v
  - Spin-Zeeman: ΔE_s
- We find the valley g-factor g_v to be of the order of 10, consistent with literature

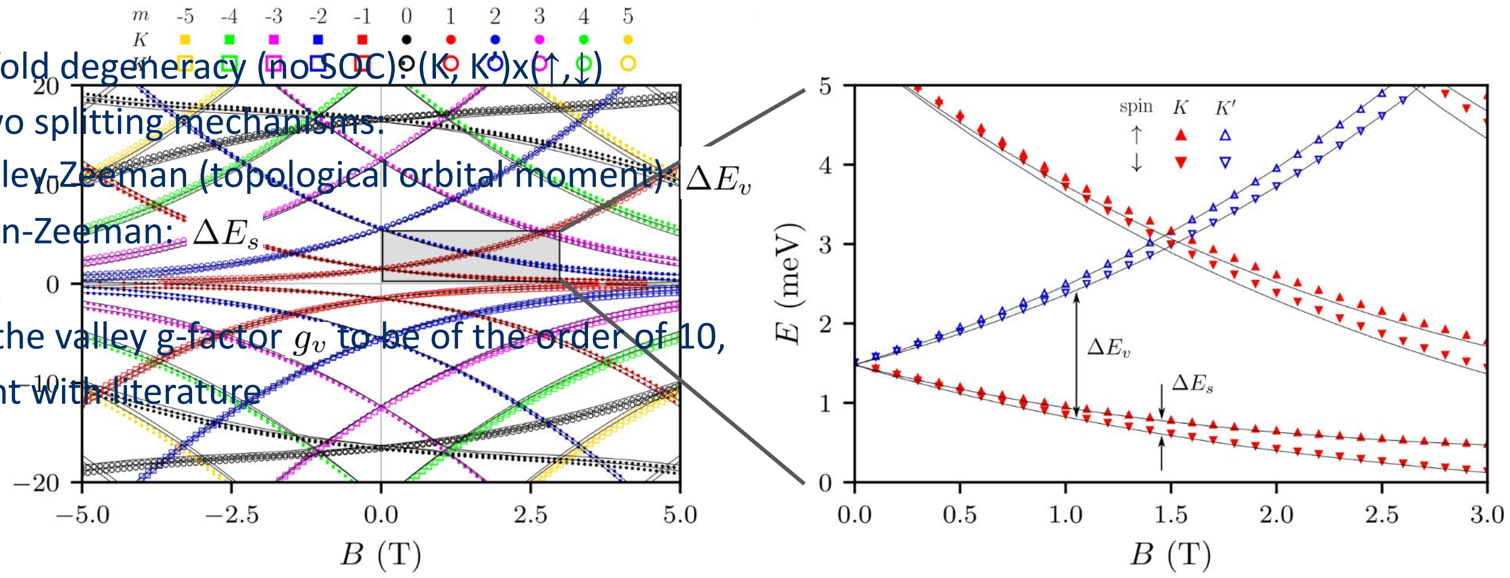

Universiteit Antwerpen

Proximitized BLG QD: energy levels vs B-field

No SOC

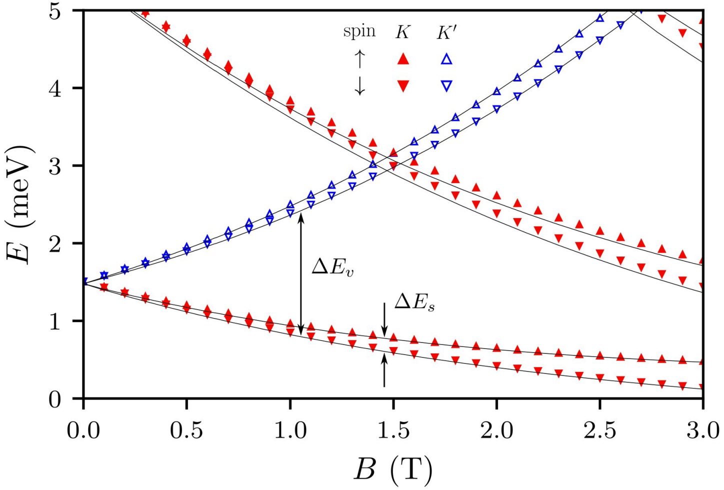

Enhanced SOC

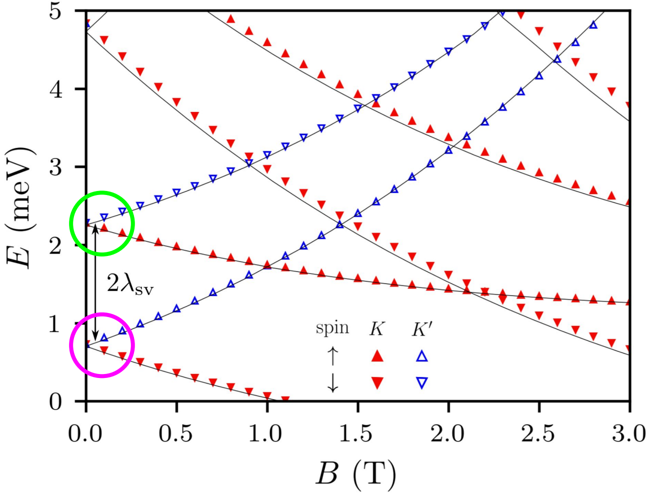

- B = 0: spin-valley coupling: spin splitting, in opposite direction K and K’
  $\longrightarrow$ Two 2-fold degeneracies: **Kramer’s pairs**: $\boxed{\{|K,\uparrow\rangle, |K',\downarrow\rangle\}}$ & $\boxed{\{|K,\downarrow\rangle, |K',\uparrow\rangle\}}$
- B ≠ 0: Completely (strongly) split energy levels $\longrightarrow$ multitude of crossings at lower B-fields

Positive vs negative energy levels

- Positive levels are spin-valley split by a factor of $2\lambda_{\mathrm{sv}}$
- Negative levels experience significantly smaller splitting
- This discrepancy is explained by their layer localization:
    - Positive levels are localized in the proximitized graphene layer, negative levels are not
- Why is there a layer bias?
    - Confining mass term potential acts as a large electric field for these low energy levels

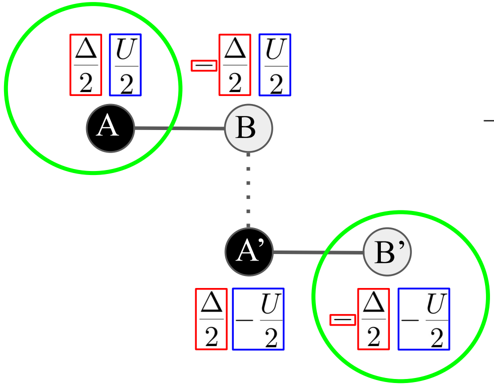

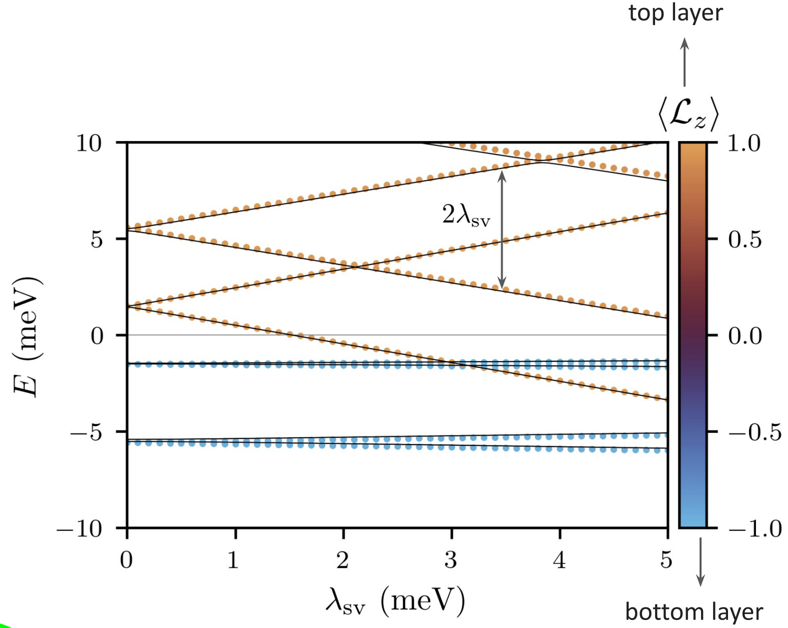

U = 0, Δ ≠ 0

Applying a transverse electric field

- Low energy states that are already layer-localized for U = 0 due to Δ
    - Layer-loc doesn't change much
    - Strong linear shift of the energy levels
        - U > 0: increase in electron-hole gap
        - U < 0: gap closing, switch of layer-localized levels

- Higher energy states without strong layer-bias at U = 0
    - Become more layer-localized and change their slope according to the sign of U

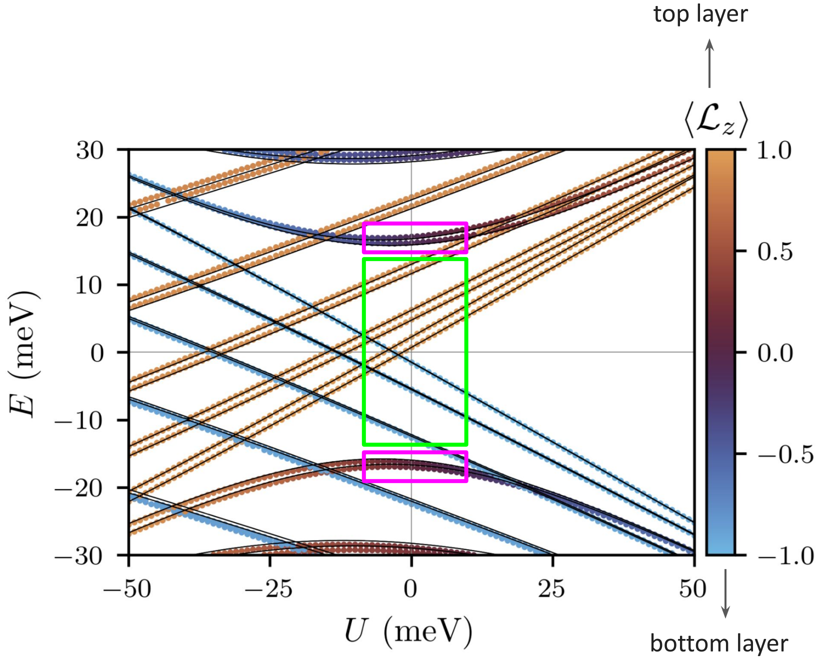

Conclusions

- BLG QD: attractive system for research and a **promising platform** for spin and valley based quantum devices
- We provided the **first theoretical description** of a proximitized BLG QD, using two models
  - Atomistic accurate tight-binding model
  - Minimal fast semi-analytical continuum model

  } well matching results
- Qualitative **agreement with experiments**: strong valley splitting, Kramer's pair splitting, tunable SOC through layer DOF + E-field
- QD energy **levels can be modified on demand** using experimentally tunable parameters, with the ability to break, as well as create degeneracies between states of different possible combinations of the quantum numbers, m, valley and spin. → qubits
- This work provides a **toolkit** to further explore the behavior of a BLG QD beyond what is shown here: e.g. QD geometries, disorder, or Rashba SOC

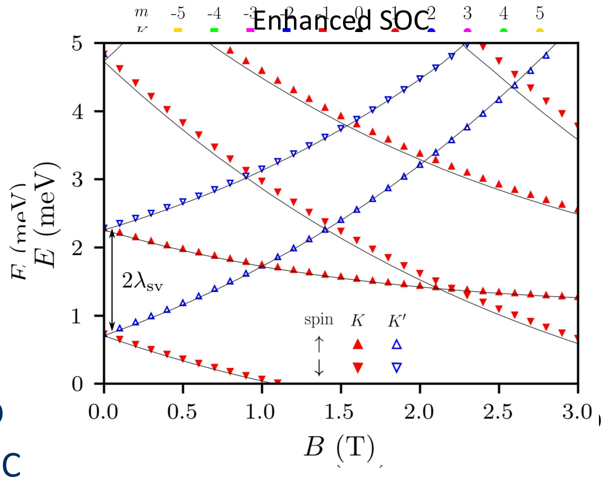

Thank you!

SOC-Hamiltonian

- For each graphene layer separately (no interlayer hoppings)
- Derived from symmetry considerations
- Graphene + TMD ⟶ 2 **broken** symmetries:
  - Space-inversion symmetry: sublattices A and B inequivalent
  - Horizontal reflection symmetry

⇒ point group reduction: $D_{6h} \longrightarrow C_{3v}$

- General C_{3v} SOC-Hamiltonian:

$$H_{\mathrm{SOC}} = \overbrace{\boxed{\frac{i}{3\sqrt{3}} \sum_{\langle\langle i,j \rangle\rangle} v_{ij} \left(\lambda_A \, \hat{a}_i^\dagger s_z \hat{a}_j + \lambda_B \, \hat{b}_i^\dagger s_z \hat{b}_j \right)}}^{H_{\mathrm{int}}} + \overbrace{\boxed{\frac{2i}{3} \sum_{\langle i,j \rangle} \left[\lambda \, \hat{a}_i^\dagger \left(\boldsymbol{s} \times \boldsymbol{d}_{ij} \right)_z \hat{b}_j + (b \leftrightarrow a) \right]}}^{H_{\mathrm{R}}}$$

$$\cancel{+ \frac{2i}{3} \sum_{\langle\langle i,j \rangle\rangle} \left[\lambda_{nn}^A \, \hat{a}_i^\dagger \left(\boldsymbol{s} \times \boldsymbol{d}_{ij} \right)_z \hat{a}_j + \lambda_{nn}^B \, \hat{b}_i^\dagger \left(\boldsymbol{s} \times \boldsymbol{d}_{ij} \right)_z \hat{b}_j \right],}$$

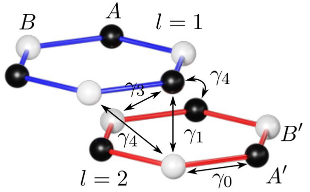

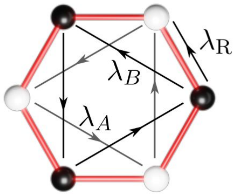

Confinement: geometry

Tight-binding

- Hexagonal flake
- Armchair edges
- QD: $\Delta(r) = \begin{cases} \Delta_0, & r > R \\ 0, & r < R \end{cases}$

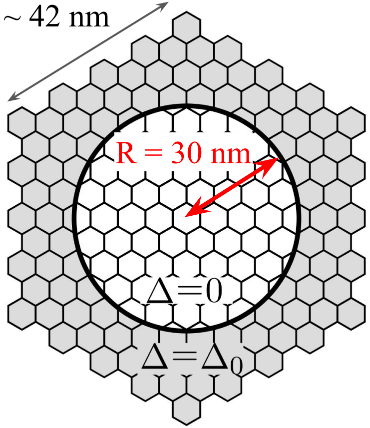

- Choosing Δ_0 :

Large: emulate infinite mass boundary condition & suppress wavefunctions outside QD

VS

Small: suppress intervalley scattering at QD edge

Continuum

$$\Delta(\rho) = \begin{cases} \Delta_0, & 1-\delta \le \rho \le 1+\delta \\ 0, & \text{otherwise} \end{cases}$$

$|\Delta_0| \to \infty$ and $\delta \to 0$

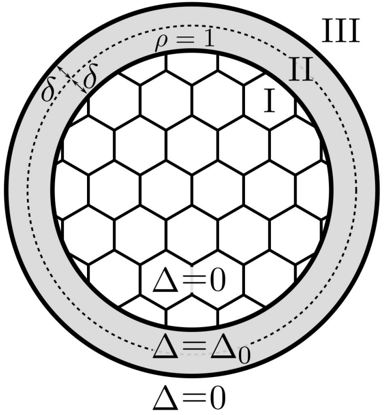

Boundary condition the spinor components:

$$\left[\phi^{(\mathrm{I})}_{4s\tau} + i\tau_{\Delta_0}\phi^{(\mathrm{I})}_{2s\tau} - i\phi^{(\mathrm{I})}_{1s\tau} + \tau_{\Delta_0}\phi^{(\mathrm{I})}_{3s\tau}\right]\Big|_{\rho=1} = 0$$

$$\left[\phi^{(\mathrm{I})}_{4s\tau} - i\tau_{\Delta_0}\phi^{(\mathrm{I})}_{2s\tau} + i\phi^{(\mathrm{I})}_{1s\tau} + \tau_{\Delta_0}\phi^{(\mathrm{I})}_{3s\tau}\right]\Big|_{\rho=1} = 0$$

$$\tau_{\Delta_0} = \tau\ \mathrm{sgn}(\Delta_0)$$